Ordered mesostructured mixed metal oxides: microporous VPO phases for *n*-butane oxidation to maleic anhydride

Moises A. Carreon[a], Vadim V. Guliants[a,*], Francesca Pierelli[b], and Fabrizio Cavani[b]

[a]*Department of Chemical and Materials Engineering, University of Cincinnati, Cincinnati, OH 45221-0012, USA*
[b]*Department of Industrial Chemistry and Materials, University of Bologna, Viale Risorgimento 4, 40136 Bologna, Italy*

Received 14 August 2003; accepted 28 October 2003

High surface area (~250 m^2/g) microporous VPO phases were prepared from the VPO/surfactant mesophases by a two-step postsynthesis treatment, consisting of a Soxhlet extraction and thermal activation in reducing atmosphere at 400 °C. The resultant microporous VPO phases were studied in the partial oxidation of *n*-butane to maleic anhydride.

KEY WORDS: mesostructured mixed oxides; microporous VPO; postsynthesis treatment; high surface area; *n*-butane oxidation.

1. Introduction

Ordered mesoporous metal oxides obtained in the presence of surfactant arrays and block copolymers are highly promising catalytic systems because of their high surface areas and enhanced rates of molecular transport of reactants and products. Despite the success of these supramolecular templating approaches for simple oxides, e.g., SiO_2, they are yet to be established as comprehensive methods of introducing desired bulk and surface structures, chemical compositions and porosities in *mixed* metal oxides, such as the vanadium phosphorus oxide (VPO) system for selective oxidation of *n*-butane to maleic anhydride (MA) [1–3]. Several examples of mesostructured VPO phases prepared using the supramolecular templating approaches have been reported [4–7]. However, only thermally unstable, low surface area and phosphorus-deficient phases were obtained. Recently, we reported the preparation of mesostructured VPO phases employing various surfactant functionalities (i.e. cationic, anionic and neutral) [8]. The complete template removal and achievement of enhanced thermal stability in this mixed metal oxide system is challenging. We have found that it was possible to remove most of the template occluded in the mesopores by using a two-step postsynthesis treatment, leading to the formation of microporous mesostructured materials. In this communication, we report for the first time the preparation of high surface area mesostructured VPO phases and their catalytic properties in *n*-butane oxidation to maleic anhydride.

* To whom correspondence should be addressed.
Email: Vadim.Guliants@uc.edu

2. Experimental

Mesostructured VPO was prepared under mild synthesis conditions [8]. In a typical preparation, 4 g of $VOSO_4$ and 2.71 g of H_3PO_3 were dissolved in 60 g of deionized water. An aqueous surfactant solution (4.94-g MTAB in 50-g water) was added to the vanadium–phosphorus source solution. The clear blue sol was homogenized at 333 K under vigorous stirring for ~2 h, then the pH was adjusted with NH_4OH (1 M) to 2.92. At this point, a greyish-blue precipitate was formed. After 16 h of stirring, the precipitate was washed with water and dried at room temperature. This as-synthesized mesostructured VPO phase was then treated by a two-step postsynthesis method: Soxhlet extraction in toluene (3–7 days) followed by thermal activation in nitrogen at 673–723 K for 8 h.

The kinetic studies were carried out in a glass flow microreactor operating at atmospheric pressure using 0.6 g of catalyst with particle dimensions in the 0.3–0.5 mm range and 1.7 vol% *n*-butane in air as feed, and the weight-to-flow rate (W/F) ratio of 1.3 $g/s/cm^3$. The space velocity in all experiments remained constant ($F/V = 55\ min^{-1}$). The products were analyzed by gas chromatography. The carbon balances based on *n*-butane conversions agreed within 5 mol%. The post-treated VPO phases were equilibrated in *n*-butane/airstream under reaction conditions at 400 °C for ~70 h.

3. Results and discussion

The general synthesis conditions, specific surface areas and largest *d*-spacings of different posttreated VPO phases are summarized in table 1. When H_3PO_3 was used as the phosphorus source, the V(IV)P(III)O phases with high surface areas were obtained. In the case

1011-372X/04/0100–0011/0

Table 1
Synthesis conditions, specific BET surface areas and largest *d*-spacings for posttreated microstructured VPO phases

Sample	Synthesis conditions	Soxhlet extraction time (h)	N_2 heat treatment[a] (K)	S.S.A. (m^2/g)	*d*-spacing (Å)
1	$VOSO_4/H_3PO_3/pH = 2.88/C_{14}TAB$	66	673	189	40.0
2	$VOSO_4/H_3PO_3/pH = 2.92/C_{14}TAB$	66	723	157	36.2
3	$VOSO_4/H_3PO_4/pH = 3.10/C_{14}TAB$	164	673	65	35.0
4	$VOSO_4/H_3PO_4/pH = 3.10/C_{14}TAB$	164	723	73	34.6
5	$VOSO_4/H_3PO_3/pH = 3.01/C_{14}TAB$	118	673	249	38.5
6	$VOSO_4/H_3PO_4/pH = 5.10$/Monododecyl phosphate	72	673	53	Amorphous

[a]8 h at 3.33 °C/min, N_2 flow rate = 40 cc/min.

of H_3PO_4, the surface areas of the V(IV)P(V)O phases were lower due to the stronger interaction of charged phosphate groups with the cationic surfactant, leading to the partial collapse of the mesostructure during template removal.

The XRD patterns (Siemens D-500 diffractometer) of the fresh and posttreated samples are shown in figure 1. The fresh sample (figure 1(a)) showed three intense peaks corresponding to the (100), (110) and (300) planes of the 2D hexagonal phase with an average unit cell parameter $a = 4.65$ nm. The posttreated sample (figure 1(b)) showed the presence of a well-defined peak at *d*-spacing = 3.85 nm, corresponding to the unit cell parameter $a = 4.44$ nm of the 2D hexagonal phase and indicating that the VPO mesostructure was retained after the two-step treatment. The shift of the main diffraction peak from 4.44 to 3.85 nm indicated an ~12.5% shrinkage of the inorganic framework due to template removal. There was a partial loss of long-range order of the 2D hexagonal phase manifested in the disappearance of the (110) and (300) reflections. The XRD patterns collected at high 2θ angles indicated the absence of dense VPO phases in both as-synthesized and

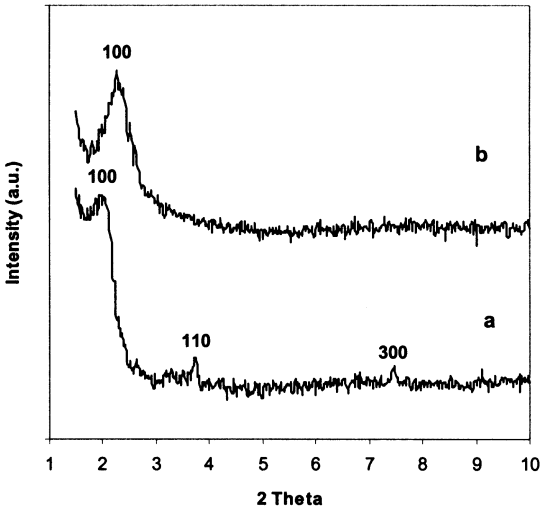

Figure 1. XRD patterns of (a) fresh and (b) posttreated micro-mesostructured VPO.

posttreated mesostructured VPO phases [2]. The bulk composition by ICP (Thermo Jarrell Ash ICAP 1100) of the posttreated samples was $P/V \sim 1.08$, which is optimal for selective oxidation of *n*-butane [1–3]. The phosphorus oxidation state in the phosphite-derived VPO phases was +5 after kinetic studies in the oxygen-containing feed.

The nitrogen adsorption–desorption isotherms at 77 K (Micromeritics Tri-Star 3000) for the posttreated sample are shown in figure 2. Prior to these measurements, the samples were outgassed for ~3 h at 423 K. This sample showed the BET specific surface area of ~250 m^2/g (evaluated in the linear pressure range, i.e. $P/P_0 \sim 0.05$ to 0.3, according to the IUPAC recommendations) [9]. (The isotherms corresponded to the Type I, with an H3 hysteresis loop characteristic of microporous materials with slit-shaped pores [9]). The pore-size distribution data based on the desorption branch (inset in figure 2) showed two interesting features: the presence of microporosity (steep slope at <2 nm indicating pore diameters smaller than 2 nm), and a well-defined peak centered at ~3.9 nm, which is an artifact accounted for by the tensile strength effect (TSE) [10]. The TSE arises from the instability of N_2 meniscus in small pores upon desorption. This is supported by the adsorption branch showing the absence of the 3.9-nm peak and confirming the presence of only microporosity. The N_2 pore analysis suggested that the final pore structure in posttreated phases is disordered with residual, partially decomposed template residing inside the mesopores. This conclusion is further supported by the results of the TGA in air and CHN elemental analysis studies of the posttreated phases. The TGA analysis (Perkin Elmer TGA-7) indicated that ~30% of the original surfactant remained strongly bound to the inorganic VPO framework determined from the weight loss feature at 423–673 K. This result was in agreement with the results of the CHN analysis (Robertson Microlit Laboratories, Inc.), which showed that ~30% of the original carbon remained in the posttreated phases. It has been previously demonstrated [11,12] that postsynthesis treatments such as steaming, thermal treatment, etc., lead to the creation of

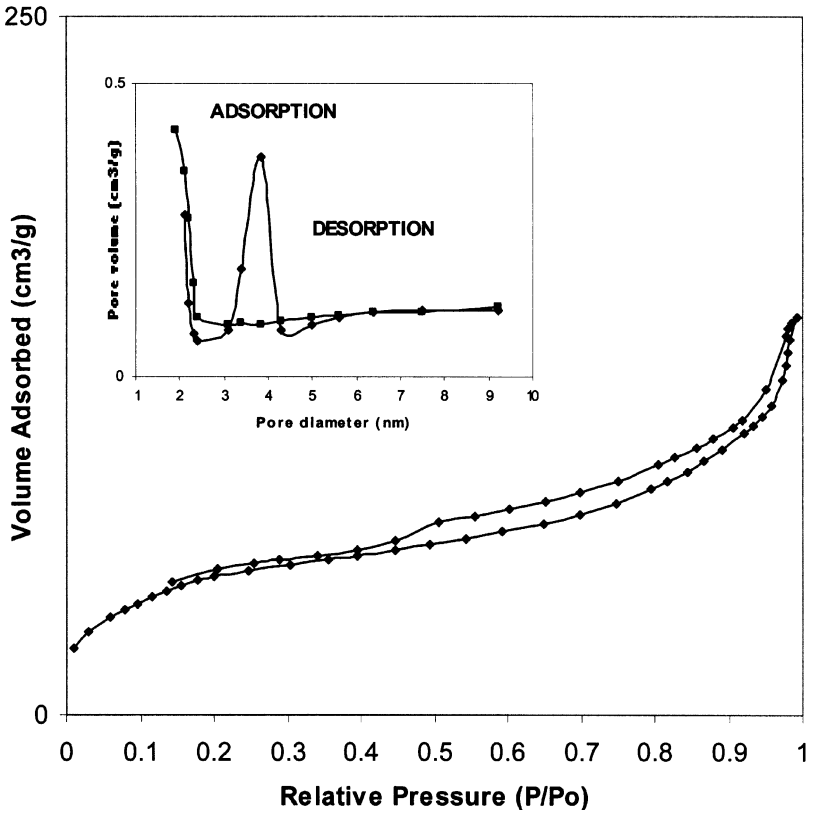

Figure 2. Nitrogen adsorption–desorption isotherms and pore-size distribution (inset) for posttreated micro-mesostructured VPO.

microporosity in various mesostructured systems. Similarly, the creation of microporosity in the posttreated phases is believed to be due to the conditions of the Soxhlet extraction process. The microporosity of posttreated phases was also confirmed at $P/P_0 < 0.05$ by the Horwath–Kawazoe (HK) method [13] using a Micromeritics ASAP 2020 pore analyzer, which demonstrated a broad micropore size distribution centered around 1.5 nm.

The theoretical surface areas ($S, \mathrm{m}^2/\mathrm{g}$) of mesostructured VPO phases were estimated for a geometrical model of a 2D hexagonal structure [14] with the unit cell parameter $a = 4.44$ nm and containing straight hexagonally shaped 1.5-nm pores according to the following equation:

$$S = \frac{11400 d_{\mathrm{pore}} \tan 30^\circ}{\rho(a^2\sqrt{3} - 0.9025 d_{pore}^2 \tan 30^\circ)}$$

where d_{pore} is the HK pore diameter (nm), a is the unit cell parameter of a 2D hexagonal structure (nm) and ρ is the wall density of the mesostructured VPO ($\mathrm{g/cm}^3$).

Assuming that the wall density in mesostructured VPO is similar to that reported for the bulk VPO phases [15] (i.e. $3.34\,\mathrm{g/cm}^3$) and a wall thickness [14] $e = a - 0.95 d_{\mathrm{pore}}$ of 3.02 nm, the theoretical surface area corresponds to $\sim 90\,\mathrm{m}^2/\mathrm{g}$. The much higher observed surface area (i.e. $250\,\mathrm{m}^2/\mathrm{g}$) is likely due to both the lower wall density of mesostructured VPO phases as well as the more complex micropore structure of mesostructured VPO phases containing occluded surfactant species.

The catalytic behavior of a typical mesostructured VPO catalyst is shown in figures 3 and 4. This particular sample was prepared as follows. An aqueous solution containing phosphorus acid and vanadyl sulfate was added to an aqueous solution of miristyl trimethyl ammonium bromide (MTAB) surfactant (Surfactant/V = 0.6). The obtained sol was homogenized by stirring for ~6 h at 333 K, precipitated with NH_4OH at pH ~ 2.90, and stirred for an additional 24 h. The resultant slurry was filtered, washed with deionized water and dried overnight at 373 K. The sample was Soxhlet-extracted with toluene for three days, and then calcined in nitrogen at 400 °C for 6 h producing a microporous mesostructured VPO phase with the specific surface area of $190\,\mathrm{m}^2/\mathrm{g}$. The bulk VPO catalysts are known to exhibit changes in catalytic behavior during the initial equilibration period on the *n*-butane/airstream [2]. Similarly, the selectivity to maleic anhydride over the mesostructured VPO catalyst increased during the first 20 h reaching a maximum value of ~40 mol% and then declined to ~30 mol% after 70 h (figure 3). However, this catalyst displayed low activity in *n*-butane oxidation (*n*-butane conversions <10 mol%) and low resulting MA yield (figure 4).

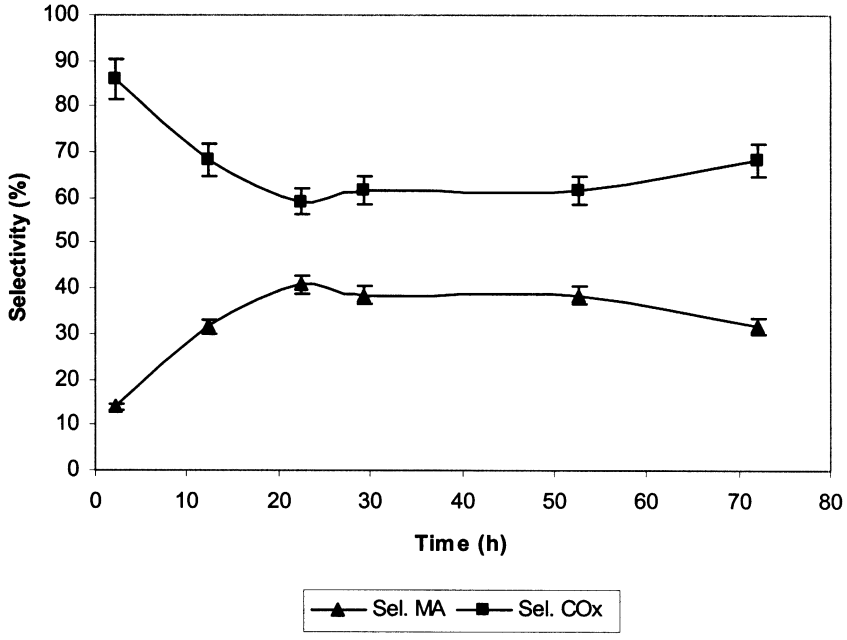

Figure 3. Catalytic performance of micro-mesostructured VPO in *n*-butane oxidation at 400 °C. Space velocity = 55 min^{-1}. Selectivity to maleic anhydride versus time.

The performance of the equilibrated mesostructured VPO catalyst as a function of temperature is shown in figures 5 and 6. The selectivities to MA of up to ~70% were observed at 460 °C (figure 5). Although the mesostructured VPO catalyst was selective to maleic anhydride, the observed low activity of this catalyst resulted in ~2 mol% yield to MA under all conditions investigated, while the conventional organic VPO catalysts under the same reaction conditions displayed the MA yields greater than 50 mol% [2]. The low MA yields observed in the case of the mesostructured VPO catalyst confirmed the critical role of the vanadyl pyrophosphate surface in catalyzing the oxidation of *n*-butane to maleic anhydride [1–3,16–19]. The reaction mechanism involved in *n*-butane oxidation is complex, and only the right combination of the surface acidic and

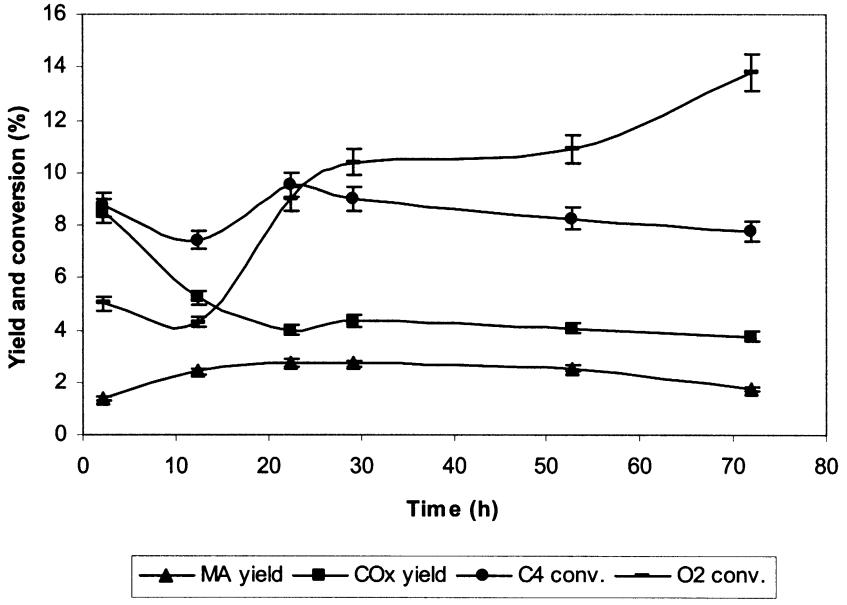

Figure 4. Catalytic performance of micro-mesostructured VPO in *n*-butane oxidation at 400 °C. Space velocity = 55 min^{-1}. Yields and conversions.

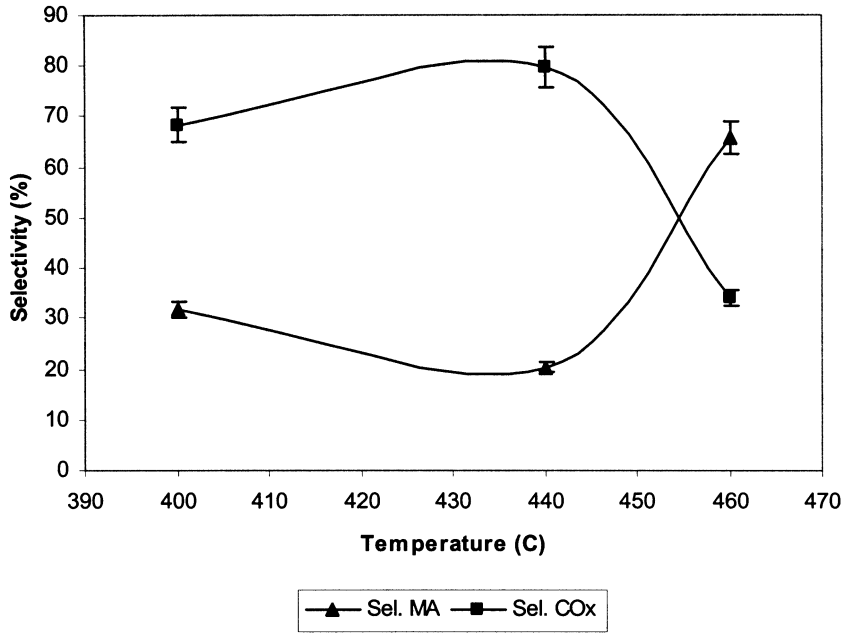

Figure 5. Selectivity to maleic anhydride and CO_X as a function of temperature. Space velocity = 55 min^{-1}.

redox sites, as in the case of $(VO)_2P_2O_7$, results in high MA selectivity and yield. Therefore, the amorphous nature of the mesostructured VPO phases as well as the presence of remaining occluded surfactant may be responsible for the observed low yield of maleic anhydride.

The mesostructured VPO phases were not thermally stable under the catalytic reaction conditions. The BET surface area measurements of the mesostructured VPO catalyst after kinetic studies indicated that the surface area decreased from 190 to 15 m^2/g. Furthermore, the XRD pattern of the mesostructured VPO catalyst after kinetic studies showed the lack of reflections at low 2θ angles. On the other hand, a number of X-ray reflections at high 2θ appeared corresponding to dense VPO phases (not shown), such as γ-$VOPO_4$ and $V(PO_3)_3$, which are less selective and active in *n*-butane oxidation to MA [2]. The incomplete cross-linking of the mesoporous VPO framework as well as its redox properties are likely responsible for the observed thermal transformation to dense VPO phases.

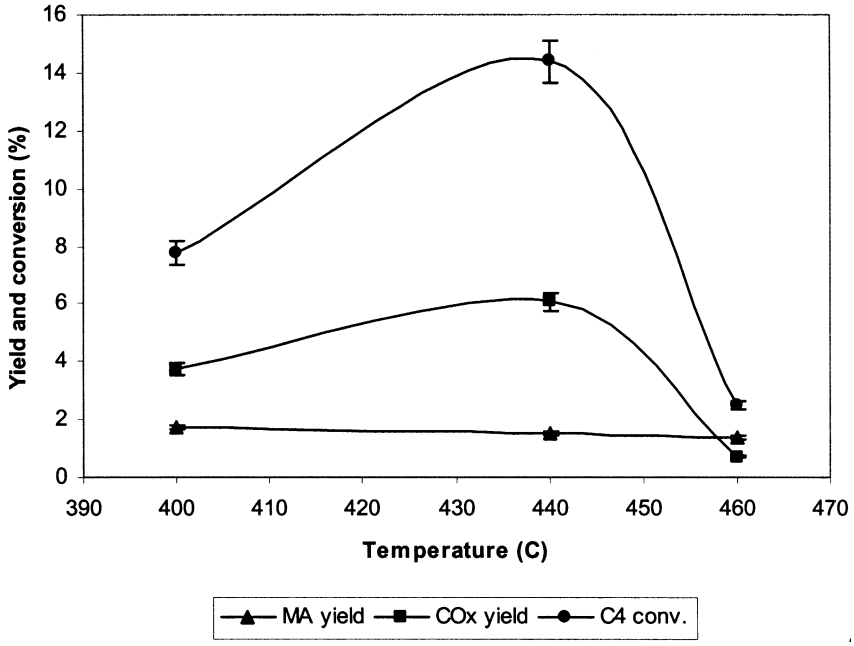

Figure 6. Conversion and yields as a function of temperature. Space velocity = 55 min^{-1}.

4. Conclusions

High surface area microporous mesostructured VPO phases were prepared from the VPO/surfactant mesophases by a two-step postsynthesis method. The catalytic behavior of these novel VPO phases were studied in the partial oxidation of *n*-butane to maleic anhydride. Although these catalysts were selective to maleic anhydride ($\sim$70 mol%) at low conversions, they transformed under catalytic reaction conditions into various dense VPO phases. Further studies to improve the thermal stability of these mixed metal oxide mesophases are underway.

Acknowledgments

V.V. Guliants acknowledges the National Science Foundation for the NSF Career Award (CTS-0238962). M.A. Carreon thanks CONACYT (Mexico) for the scholarship award.

References

[1] G. Centi, Catal. Today 5 (1993) 16.
[2] V.V. Guliants, J.B. Benziger, S. Sundaresan, I.E. Wachs, J.M. Jehng and J.E. Roberts, Catal. Today 28 (1996) 275.
[3] F. Trifiró, Catal. Today 21 (1998) 41.
[4] T. Abe, A. Taguchi and M. Iwamoto, Chem. Mater. 7 (1995) 1429.
[5] T. Doi and T. Miyake, Chem. Commun. (1996) 1635.
[6] J.E. Haskouri, M. Roca, S. Cabrera, J. Alamo, A. Beltran-Porter, D. Beltran-Porter, M.D. Marco and P. Amoros, Chem. Mater. 11 (1999) 1446.
[7] N. Mizuno, H. Hatayama, S. Uchida and A. Taguchi, Chem. Mater. 13 (2001) 179.
[8] M.A. Carreon and V.V. Guliants, Microporous Mesoporous Mater. 55 (2002) 297–304.
[9] K.S.W. Sing, D.H. Everett, R.A.W. Haul, L. Moscou, R.A. Pierrotti, J. Rouquerol and T. Siemieniewska, Pure Appl. Chem. 57 (1985) 603.
[10] J.C. Groen, L.A.A. Peffer and J. Perez-Ramirez, Microporous Mesoporous Mater. 51 (2002) 75.
[11] M.S. Wong and J.Y. Ying, Chem. Mater. 10 (1998) 2067.
[12] M. Imperor-Clerc, P. Davidson and A. Davidson, J. Am. Chem. Soc. 122 (2000) 11925.
[13] G. Horvath and K. Kawazoe, J. Chem. Eng. Jpn. 16 (1983) 470.
[14] A. Galarneau, D. Desplantier, R. Dutartre and F. Di Renzo, Microporous Mesoporous Mater. 27 (1999) 297.
[15] P.T. Nguyen, R.D. Hoffman and A.W. Sleight, Mater. Res. Bull. 30 (1995) 1055.
[16] G. Centi, F. Cavani and F. Trifiró, *Selective Oxidation by Heterogeneous Catalysis. Fundamental and Applied Catalysis* (Kluwer Academic-Plenum Publishers, 2001).
[17] G. Centi, F. Trifiró, J.R. Ebner and V.M. Franchetti, Chem. Rev. 88 (1988) 55.
[18] R.M. Contractor, J.R. Ebner and M.J. Mummy, in *New Developments in Selective Oxidation*, G. Centi and F. Trifiró (eds) (Elsevier, Amsterdam, 1990).
[19] E. Bordes, Catal. Today 16 (1993) 27.